



## Wnt Stabilization of $\beta$ -Catenin Reveals Principles for Morphogen Receptor-Scaffold Assemblies

Sung-Eun Kim *et al.*

*Science* **340**, 867 (2013);

DOI: 10.1126/science.1232389

*This copy is for your personal, non-commercial use only.*

If you wish to distribute this article to others, you can order high-quality copies for your colleagues, clients, or customers by [clicking here](#).

Permission to republish or repurpose articles or portions of articles can be obtained by following the guidelines [here](#).

**The following resources related to this article are available online at [www.sciencemag.org](http://www.sciencemag.org) (this information is current as of July 27, 2013):**

**Updated information and services**, including high-resolution figures, can be found in the online version of this article at:

<http://www.sciencemag.org/content/340/6134/867.full.html>

**Supporting Online Material** can be found at:

<http://www.sciencemag.org/content/suppl/2013/04/10/science.1232389.DC1.html>

A list of selected additional articles on the Science Web sites **related to this article** can be found at:

<http://www.sciencemag.org/content/340/6134/867.full.html#related>

This article **cites 39 articles**, 14 of which can be accessed free:

<http://www.sciencemag.org/content/340/6134/867.full.html#ref-list-1>

This article appears in the following **subject collections**:

Cell Biology

[http://www.sciencemag.org/cgi/collection/cell\\_biol](http://www.sciencemag.org/cgi/collection/cell_biol)

autoinhibition was released inside the nucleus, which suggests that nuclear formin regulation is dynamically and tightly controlled. Thus, the entire process from actin polymerization to SRF-dependent gene expression can occur in the nucleus. Moreover, nuclear formin function represents an integral part of the physiological serum response.

#### References and Notes

1. C. Baarlink, D. Brandt, R. Grosse, *Cell* **142**, 172, 172e1 (2010).
2. J. Faix, R. Grosse, *Dev. Cell* **10**, 693 (2006).
3. S. H. Zigmond, *Curr. Opin. Cell Biol.* **16**, 99 (2004).
4. T. Miki *et al.*, *J. Biol. Chem.* **284**, 5753 (2009).
5. T. Stüven, E. Hartmann, D. Görlich, *EMBO J.* **22**, 5928 (2003).
6. S. Arsenian, B. Weinhold, M. Oelgeschläger, U. Rütger, A. Nordheim, *EMBO J.* **17**, 6289 (1998).
7. E. N. Olson, A. Nordheim, *Nat. Rev. Mol. Cell Biol.* **11**, 353 (2010).

8. M. K. Vartiainen, S. Guettler, B. Larjani, R. Treisman, *Science* **316**, 1749 (2007).
9. S. J. Copeland *et al.*, *J. Biol. Chem.* **282**, 30120 (2007).
10. S. Stern *et al.*, *J. Neurosci.* **29**, 4512 (2009).
11. F. Miralles, G. Posern, A.-I. Zaromytidou, R. Treisman, *Cell* **113**, 329 (2003).
12. S. B. Padrick, M. K. Rosen, *Annu. Rev. Biochem.* **79**, 707 (2010).
13. J. W. Copeland, R. Treisman, *Mol. Biol. Cell* **13**, 4088 (2002).
14. R. S. Gieni, M. J. Hendzel, *Biochem. Cell Biol.* **87**, 283 (2009).
15. B. M. Jockusch, C.-A. Schoenenberger, J. Stetefeld, U. Aebi, *Trends Cell Biol.* **16**, 391 (2006).
16. M. K. Vartiainen, *FEBS Lett.* **582**, 2033 (2008).
17. T. J. Gauvin, J. Fukui, J. R. Peterson, H. N. Higgs, *Biochemistry* **48**, 9327 (2009).
18. D. R. Kovar, *Curr. Opin. Cell Biol.* **18**, 11 (2006).
19. A. S. Alberts, *J. Biol. Chem.* **276**, 2824 (2001).
20. S. M. Harper, L. C. Neil, K. H. Gardner, *Science* **301**, 1541 (2003).

**Acknowledgments:** We thank J. V. Small for advice on rapid actin fixation, L. O. Essen and C. Taxis for advice on using the LOV-domain, M. Innocenti for mDia2 antibodies, B. Di Ventura for critical reading of the manuscript, and laboratory members for discussions. This work was funded by grants from the Deutsche Forschungsgemeinschaft (GR 2111/2-1 and SFB 593) and the Deutsche Krebshilfe e.V. (108293) to R.G. The data presented in this manuscript are tabulated in the main paper and in the supplementary materials.

#### Supplementary Materials

www.sciencemag.org/cgi/content/full/science.1235038/DC1  
Materials and Methods  
Figs. S1 to S8  
References (21–24)  
Movies S1 to S4

11 January 2013; accepted 26 March 2013  
Published online 4 April 2013;  
10.1126/science.1235038

# Wnt Stabilization of $\beta$ -Catenin Reveals Principles for Morphogen Receptor-Scaffold Assemblies

Sung-Eun Kim,<sup>1\*</sup> He Huang,<sup>1,\*†</sup> Ming Zhao,<sup>2\*</sup> Xinjun Zhang,<sup>1</sup> Aili Zhang,<sup>2,4</sup> Mikhail V. Semonov,<sup>1,‡</sup> Bryan T. MacDonald,<sup>1</sup> Xiaowu Zhang,<sup>5</sup> Jose Garcia Abreu,<sup>1,3</sup> Leilei Peng,<sup>2</sup> Xi He<sup>1§</sup>

Wnt signaling stabilizes  $\beta$ -catenin through the LRP6 receptor signaling complex, which antagonizes the  $\beta$ -catenin destruction complex. The Axin scaffold and associated glycogen synthase kinase-3 (GSK3) have central roles in both assemblies, but the transduction mechanism from the receptor to the destruction complex is contentious. We report that Wnt signaling is governed by phosphorylation regulation of the Axin scaffolding function. Phosphorylation by GSK3 kept Axin activated (“open”) for  $\beta$ -catenin interaction and poised for engagement of LRP6. Formation of the Wnt-induced LRP6-Axin signaling complex promoted Axin dephosphorylation by protein phosphatase-1 and inactivated (“closed”) Axin through an intramolecular interaction. Inactivation of Axin diminished its association with  $\beta$ -catenin and LRP6, thereby inhibiting  $\beta$ -catenin phosphorylation and enabling activated LRP6 to selectively recruit active Axin for inactivation reiteratively. Our findings reveal mechanisms for scaffold regulation and morphogen signaling.

Signaling by secreted Wnt morphogens governs developmental, homeostatic, and pathological processes by regulating  $\beta$ -catenin stability and represents a critical target for cancer and disease therapeutics (1, 2). Without Wnt stimulation, cytosolic  $\beta$ -catenin concentrations are kept low because a “destruction complex” assembled by the Axin scaffold binds to  $\beta$ -catenin, Adenomatous polyposis coli (APC), casein kinase-1 $\alpha$  (CK1 $\alpha$ ), and glycogen synthase

kinase-3 (GSK3), and promotes phosphorylation of  $\beta$ -catenin by CK1 $\alpha$  and GSK3, thus ensuring  $\beta$ -catenin ubiquitination and degradation (1–3). Upon Wnt stimulation, a receptor complex on the cell surface is formed between Frizzled (Fz) and low-density lipoprotein receptor-related protein 6 (LRP6), resulting in phosphorylation and activation of LRP6 and its recruitment of Axin (4–7). Assembly of the Fz-LRP6 complex and associated Dishevelled (Dvl) and the Axin destruction complex, referred to collectively as the LRP6 signaling complex (signalosome), inhibits phosphorylation of  $\beta$ -catenin, thereby causing its stabilization (6–10). The mechanism by which LRP6 activation leads to  $\beta$ -catenin stabilization remains enigmatic (1, 2, 11).

Axin is a phosphoprotein central to assemblies of both destruction (12–15) and signaling complexes (4–10), and it becomes dephosphorylated upon Wnt stimulation (16, 17). We generated an antibody, Ab-pS497/500 (fig. S1, A to C), for Axin phosphorylated at serines 497 and 500, which are GSK3 phosphorylation sites in vitro (18). Axin phosphorylation at S497/S500 was decreased within 15 to 30 min of Wnt3a treatment of mouse L fibroblasts (Fig. 1A), embryonic fibroblasts (fig. S1D), and human embryonic kidney (HEK) 293T cells (Fig. 1, C and D). Wnt-induced dephosphorylation of Axin likely reflects the counterbalance between GSK3 and a protein phosphatase (PP) such as PP1, whose catalytic subunit, PP1c, was identified in an RNA interference screen in *Drosophila* cells as a requirement for Wnt/ $\beta$ -catenin signaling (19). Through a functional cDNA overexpression screen in HEK293T cells, we identified PP1 $\gamma$ , one of the three PP1c genes in the human genome (20), as an activator of the Wnt/ $\beta$ -catenin signaling reporter TOP-Flash (fig. S2A). PP1 $\gamma$  overexpression decreased phosphorylation of Axin but not of LRP6 (Fig. 1B); a pharmacological PP1 inhibitor, Tautomycin (TM), prevented Wnt-induced dephosphorylation of Axin without affecting LRP6 phosphorylation (Fig. 1C and fig. S3).

PP1 has pleiotropic roles, and its specificity is conferred by hundreds of PP1c-binding proteins (20). Inhibitor-2 (I2, or PPP1R2) is a specific inhibitor of PP1c (20). Overexpression of I2 countered Wnt3a-induced Axin dephosphorylation (without affecting LRP6 phosphorylation) and  $\beta$ -catenin stabilization (Fig. 1D and fig. S2B), inhibited Wnt3a- or PP1 $\gamma$ -activated TOP-Flash (fig. S2, C and D), and antagonized  $\beta$ -catenin stabilization by an activated LRP6 (fig. S2E). Depletion of the endogenous I2 with short hairpin RNAs (shRNAs) resulted in accumulation of  $\beta$ -catenin and increased TOP-Flash (Fig. 1E and fig. S2F). A morpholino antisense oligonucleotide (MO) that targets *Xenopus* I2 mRNA and blocked I2 protein synthesis caused deficiency in *Xenopus* head development and reduced anterior marker expression, which were restored by human I2 mRNA injection or knockdown of  $\beta$ -catenin (Fig. 1F and fig. S4). Thus, I2 antagonizes Wnt/ $\beta$ -catenin signaling and participates in vertebrate anteriorization, which requires Wnt pathway inhibition (21).

Recent models of Wnt signaling (22, 23) have overlooked Axin phosphorylation, and one

<sup>1</sup>F. M. Kirby Center, Boston Children’s Hospital, Harvard Medical School, Boston, MA 02115, USA. <sup>2</sup>College of Optical Sciences, University of Arizona, Tucson, AZ 85721, USA. <sup>3</sup>Instituto de Ciencias Biológicas, Universidade Federal do Rio de Janeiro, Rio de Janeiro, Brazil. <sup>4</sup>School of Biomedical Engineering, Jiaotong University, Shanghai, China. <sup>5</sup>Cell Signaling Technology, Danvers, MA 01923, USA.

\*These authors contributed equally to this work.

†Present address: Department of Pathology, University of Buffalo, Buffalo, NY 14203, USA.

‡Present address: Veterans Administration Hospital and Department of Pathology, Boston University, Bedford, MA 01730, USA.

§Corresponding author. E-mail: xi.he@childrens.harvard.edu

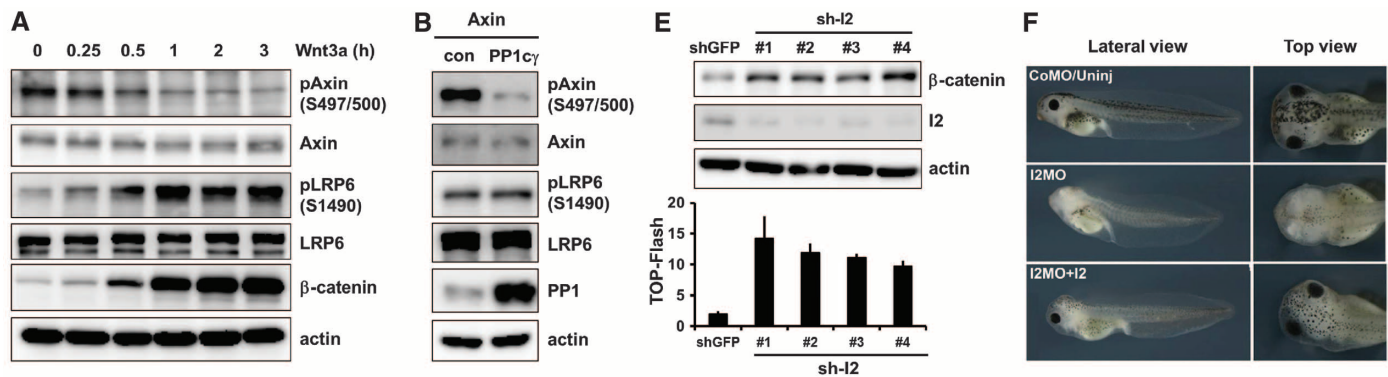


**Fig. 1. Wnt-induced Axin dephosphorylation by PP1 and effects of I2 on Wnt signaling and *Xenopus* anteriorization.** (A) Wnt3a-induced Axin dephosphorylation, LRP6 phosphorylation and  $\beta$ -catenin stabilization in L cells. Protein detections were performed by immunoblotting throughout the paper unless specified otherwise. actin, a loading control. (B) Effect of PP1 $\gamma$  overexpression on phosphorylation of Axin but not LRP6 in HEK293T cells. (C and D) Effects of TM (C) or I2 overexpression (D) on Wnt3a-induced Axin dephosphorylation and  $\beta$ -catenin stabilization in HEK293T cells. (E) Effects of I2 depletion with shRNAs (sh-I2) on  $\beta$ -catenin stabilization (top) and TOP-Flash (bottom) in HEK293T cells. shGFP, an shRNA against green fluorescent protein. Error bars, mean  $\pm$  SD of triplicates. (F) Effect of I2 depletion with an I2MO in embryos and its rescue by human I2 mRNA. CoMo/Uninj, control MO-injected/uninjected.

argued that Wnt/LRP6 signaling maintains an intact Axin destruction complex without inhibiting  $\beta$ -catenin phosphorylation (22). We reevaluated this critical issue. We found that in multiple Wnt-responsive cells, the rate of  $\beta$ -catenin phosphorylation was suppressed under Wnt stimulation (fig. S5) as reported (3, 24), and this correlated with Axin dephosphorylation.

Association of Axin and  $\beta$ -catenin is the cornerstone binary interaction within the destruction complex. Coimmunoprecipitation (co-IP) of endogenous proteins showed that the amount of  $\beta$ -catenin associated with Axin appeared to be unchanged or decrease after 0.5 hours of Wnt treatment but to increase after 2 hours (fig. S6, A and B). However normalization to the amount of cytosolic  $\beta$ -catenin made it clear that Wnt stimulation weakened the interaction between  $\beta$ -catenin and Axin (Fig. 2, A and B, left panels). We estimated that the dissociation constant ( $K_d$ ) of Axin- $\beta$ -catenin association was increased by Wnt3a (fig. S6C), signifying a weaker interaction. Indeed, Axin from extracts of Wnt3a-treated cells exhibited reduced capability to associate with  $\beta$ -catenin in an *in vitro* binding assay (Fig. 3A) (17). Such diminished Axin- $\beta$ -catenin association observed *in vitro* and *in vivo* correlated with, and appeared to be attributable to, Axin dephosphorylation by PP1, because it could be partially restored by I2 overexpression or TM treatment (Fig. 3, A to C). For  $\beta$ -catenin coimmunoprecipitated with Axin from Wnt3a-treated cells, the amount of phosphorylation relative to that of  $\beta$ -catenin was reduced (Fig. 2, A and B, middle panels; and fig. S6, A and B), implying a diminished rate of  $\beta$ -catenin phosphorylation in the Axin complex in Wnt-treated cells. Association of Axin with GSK3 remained

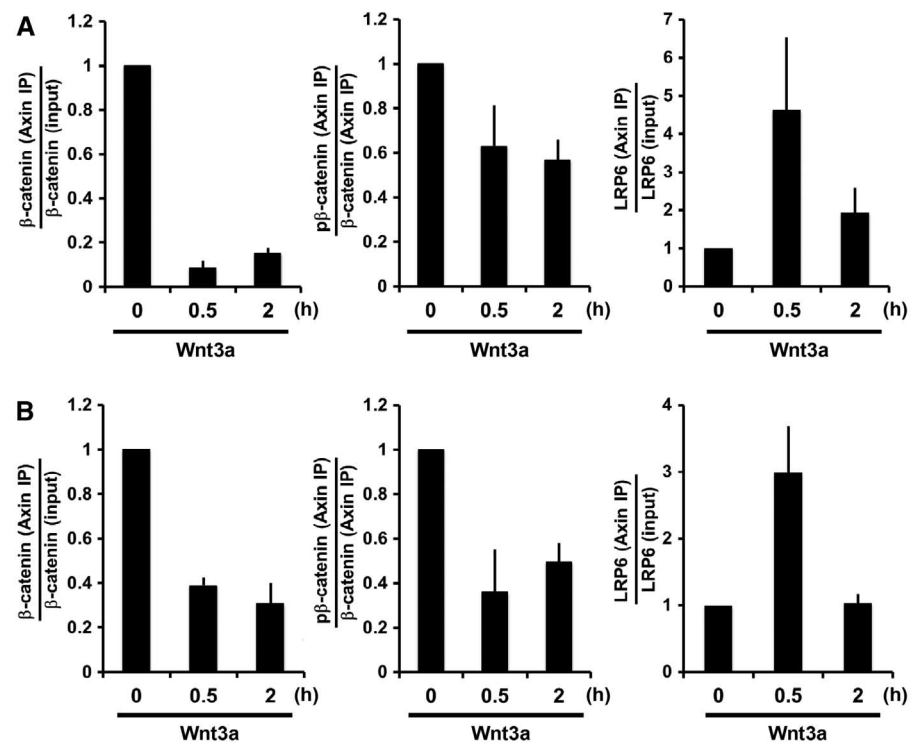


**Fig. 2. Wnt regulation of Axin- $\beta$ -catenin and Axin-LRP6 association, and of  $\beta$ -catenin phosphorylation in the Axin complex.** (A and B) Quantifications of Wnt3a effects on ratios of Axin-associated  $\beta$ -catenin versus input  $\beta$ -catenin (left), Axin-associated phospho- $\beta$ -catenin versus Axin-associated  $\beta$ -catenin (middle), and Axin-associated LRP6 versus total LRP6 (right) in L (A) and HEK293T (B) cells. Error bars, mean  $\pm$  SEM of triplicates.

constant regardless of Wnt treatment (fig. S6, A and B) (22, 25). Thus, Wnt signaling inhibits Axin- $\beta$ -catenin association and  $\beta$ -catenin phosphorylation, consistent with earlier findings

(3, 17), kinetic modeling (24), and the prevailing model (1, 11, 14, 15) (see fig. S6C).

Wnt-induced phosphorylation of LRP6 recruits Axin to assemble the signaling complex

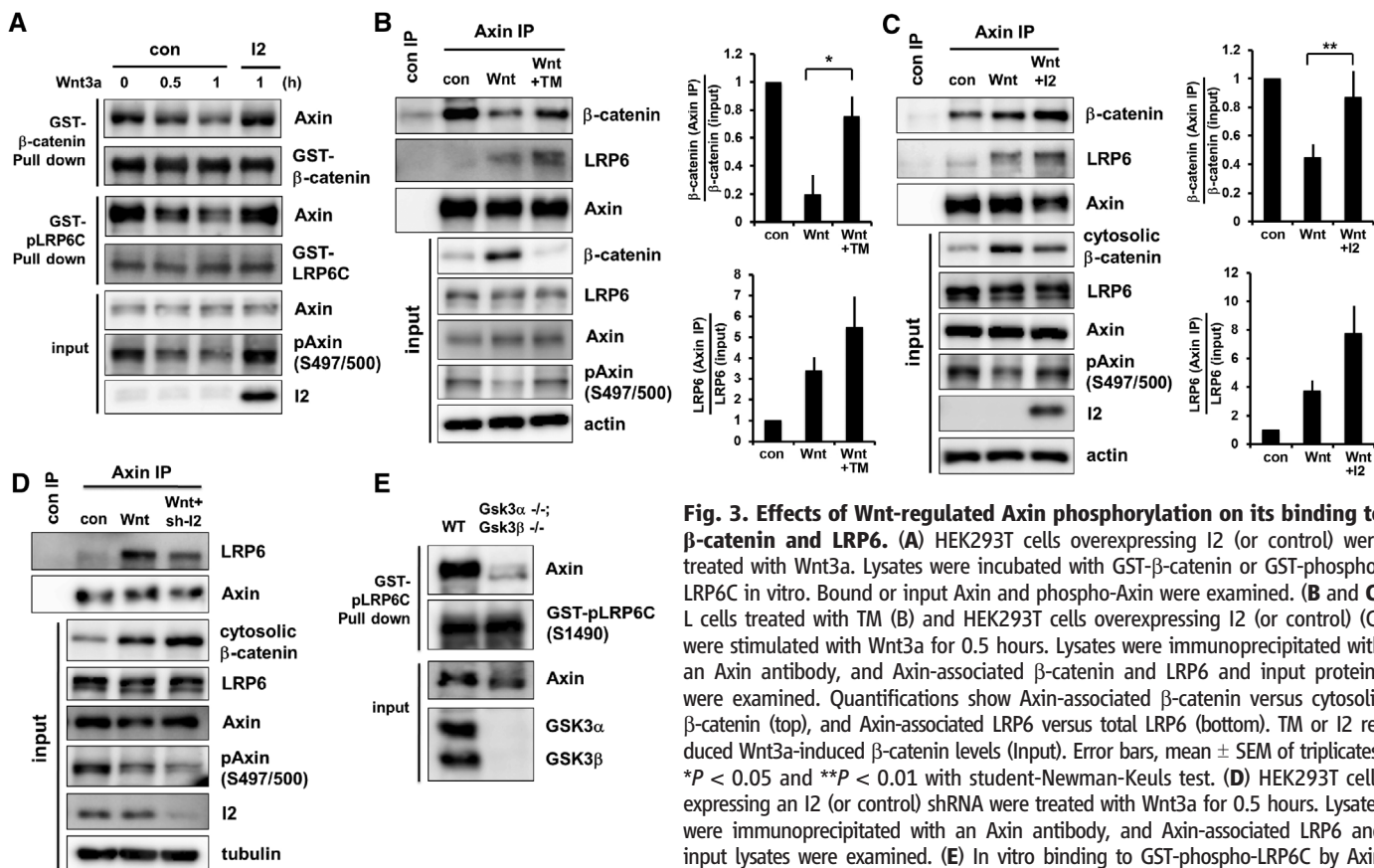


**Fig. 3. Effects of Wnt-regulated Axin phosphorylation on its binding to  $\beta$ -catenin and LRP6.** (A) HEK293T cells overexpressing I2 (or control) were treated with Wnt3a. Lysates were incubated with GST- $\beta$ -catenin or GST-phospho-LRP6C in vitro. Bound or input Axin and phospho-Axin were examined. (B and C) L cells treated with TM (B) and HEK293T cells overexpressing I2 (or control) (C) were stimulated with Wnt3a for 0.5 hours. Lysates were immunoprecipitated with an Axin antibody, and Axin-associated  $\beta$ -catenin and LRP6 and input proteins were examined. Quantifications show Axin-associated  $\beta$ -catenin versus cytosolic  $\beta$ -catenin (top), and Axin-associated LRP6 versus total LRP6 (bottom). TM or I2 reduced Wnt3a-induced  $\beta$ -catenin levels (Input). Error bars, mean  $\pm$  SEM of triplicates. \* $P < 0.05$  and \*\* $P < 0.01$  with student-Newman-Keuls test. (D) HEK293T cells expressing an I2 (or control) shRNA were treated with Wnt3a for 0.5 hours. Lysates were immunoprecipitated with an Axin antibody, and Axin-associated LRP6 and input lysates were examined. (E) In vitro binding to GST-phospho-LRP6C by Axin from lysates of WT or Gsk3 $\alpha^{-/-}$ ;Gsk3 $\beta^{-/-}$  mouse embryonic stem cells. Bound or input Axin was examined.

(5–7). Intriguingly, co-IP of endogenous proteins showed that Wnt-induced association of LRP6 and Axin was prominent at 0.5 hours but diminished after 2 hours (Fig. 2, A and B, right panels; and fig. S6, A and B), despite persistence of phospho-LRP6 (fig. S5). The diminished binding between phospho-LRP6 and Axin appeared to result from Axin dephosphorylation by PP1, because the binding was enhanced by I2 overexpression or TM treatment (Fig. 3, B and C) and reduced by I2 depletion (Fig. 3D). Axin from extracts of Wnt3a-treated cells showed reduced capability to associate with phospho-LRP6 in an in vitro binding assay (fig. S7A), and this reduction appeared to result from Axin dephosphorylation by PP1 because it was prevented by I2 overexpression (Fig. 3A). Complementarily, Axin from extracts of cells treated with a pharmacological GSK3 inhibitor, BIO or SB216763, or of Gsk3 $\alpha^{-/-}$ ;Gsk3 $\beta^{-/-}$  cells (26), had minimal association with phospho-LRP6 (Fig. 3E and fig. S7B). Thus, phosphorylation of Axin by GSK3 enhanced, whereas dephosphorylation of Axin by PP1 diminished, Axin's ability to associate with phospho-LRP6 (and  $\beta$ -catenin), implying that activated LRP6 selectively recruits the phosphorylated form of Axin that is active in  $\beta$ -catenin association and degradation.

The above results imply that Axin may undergo a phosphorylation-dependent conforma-

tional change. Axin is an intrinsically disordered protein with individual partner-binding domains (fig. S8A) (14, 15). Axin's  $\beta$ -catenin binding domain (Axin-BCD) associated, in vitro and when overexpressed in cells, with Axin DIX domain (Axin-DIX) but not homologous Dvl2 DIX domain (Dvl-DIX) (Fig. 4A and figs. S8B and S9), reflecting a specific and direct interaction. Phosphorylation of Axin-BCD by GSK3 in vitro inhibited BCD-DIX binding (Fig. 4A and fig. S8C). Therefore, there may be an intramolecular BCD-DIX interaction that is prevented upon Axin phosphorylation by GSK3, providing an explanation for how phosphorylation of Axin enhances its association with  $\beta$ -catenin and phospho-LRP6. Indeed Axin intra- and intermolecular interactions appeared to be mutually exclusive because  $\beta$ -catenin and Axin-DIX competed for binding to Axin-BCD (Fig. 4B and fig. S10A). A positively charged histidine-rich region of BCD (figs. S9, S10B, and S11) and a negatively charged loop of DIX (figs. S12A and S13) participated in BCD-DIX interaction, which appeared to be disrupted by negative charges generated in BCD through phosphorylation by GSK3 (figs. S10, C and D, and S11). Axin(SD4), which contains phosphomimetic aspartic acid substitutions of four serines (including S497 and S500) in BCD (fig. S11), and Axin(DA), which contains alanine substitutions

of acidic residues in DIX (fig. S13), were each expected to have a weaker intramolecular interaction (figs. S10D and S12A) and were indeed more effective in inhibiting Wnt/ $\beta$ -catenin signaling than the wild-type (WT) Axin (Fig. 4C). Axin(SA4), which contains alanine substitutions of the four serines in BCD (fig. S11) and was predicted to have a stronger intramolecular interaction (fig. S10C), was less effective in inhibiting Wnt/ $\beta$ -catenin signaling (Fig. 4C). These results support a model that Axin "autoinhibits" through the BCD-DIX intramolecular interaction. Live cell FRET (fluorescence resonance energy transfer) imaging corroborated this model by demonstrating a Wnt3a-induced proximity of Axin's carboxyl DIX to its amino terminus (figs. S14 to S17), likely through Axin dephosphorylation.

We propose a Wnt signaling model (Fig. 4D) that appears to unify findings on the two Axin complexes mediating LRP6 signaling and  $\beta$ -catenin destruction. Without Wnt, Axin is associated with and phosphorylated by GSK3 and is in an activated ("open") conformation for  $\beta$ -catenin binding and phosphorylation and poised for engagement of LRP6 (Fig. 4D). With Wnt, LRP6 undergoes Fz/Dvl-dependent phosphorylation and recruits the active Axin destruction complex to form the signaling complex, in which GSK3 bound to Axin is inhibited by phospho-LRP6

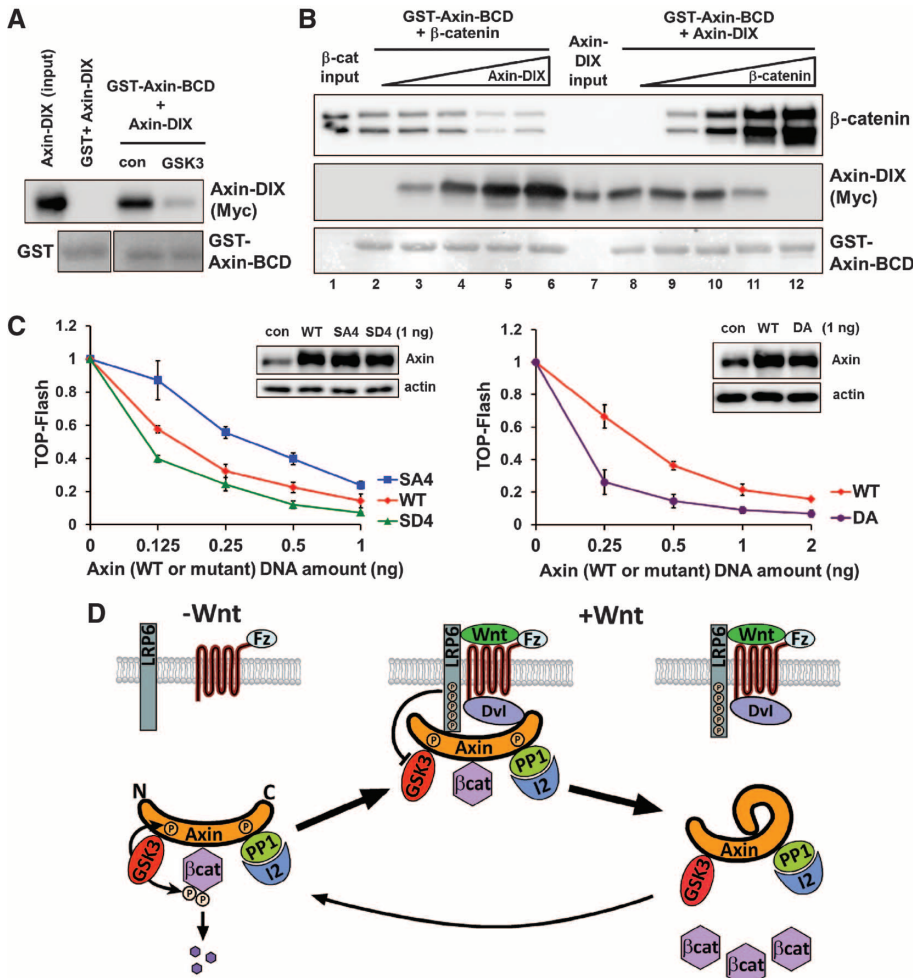


**Fig. 4. A phosphorylation-regulated Axin intramolecular interaction and its inhibition by GSK3 phosphorylation of Axin-BCD. (A)** Association of Axin-DIX with GST-Axin-BCD and its inhibition by GSK3 phosphorylation of Axin-BCD. **(B)** Competition of  $\beta$ -catenin association with GST-Axin-BCD by Axin-DIX (lanes 1 to 6) and vice versa (lanes 7 to 12). Purified recombinant proteins were used in these *in vitro* assays. Axin-DIX or  $\beta$ -catenin was detected by immunoblotting and GST or GST-Axin-BCD by Ponceau staining [(A) and (B)]. The lower band of  $\beta$ -catenin (B) was a proteolytic fragment. **(C)** Comparisons of Axin(SD4), Axin(SA4), and Axin(DA) with Axin in antagonizing Wnt-induced TOP-Flash in HEK293T cells. *x* axes represent DNA doses transfected. Error bars, mean  $\pm$  SD of triplicates. Note larger TOP-Flash differences at lower overexpression doses. Insets show levels of overexpressed Axin at the 1 ng dose and that of endogenous Axin (con). **(D)** An “Axin inactivation” model for Wnt stabilization of  $\beta$ -catenin. APC and CK1 $\alpha$  were omitted for clarity. See text and fig. S18.

(27–29), leading to inhibition of  $\beta$ -catenin phosphorylation and tipping the balance toward Axin dephosphorylation by PP1. Dephosphorylated Axin adopts an inactivated (“closed”) conformation through intramolecular autoinhibition and becomes incompetent for association with  $\beta$ -catenin or phospho-LRP6, leading to disassembly of destruction and signaling complexes (Fig. 4D). Phospho-LRP6 is thus freed for another round of recruitment of phosphorylated-activated Axin for inactivation while ignoring dephosphorylated-inactivated Axin, and the steps likely reiterate to keep  $\beta$ -catenin phosphorylation suppressed. Wnt-induced biphasic assembly and disassembly of the LRP6 signaling complex appear to enable phospho-LRP6 to inactivate Axin in a “catalytic” manner, underlying Wnt stabiliza-

tion of  $\beta$ -catenin in broad component stoichiometries. GSK3 acts as an “assembler” of destruction (16–18) and signaling complexes (4, 6, 8–10) through phosphorylation of Axin and LRP6, whereas PP1 dephosphorylates Axin (19) to disassemble both complexes while leaving phospho-LRP6 unperturbed for continuous signaling. Our model further explains  $\beta$ -catenin stabilization kinetics. Elevating levels of  $\beta$ -catenin, by competing against Axin intramolecular autoinhibition, could promote reassembly of the Axin-GSK3- $\beta$ -catenin complex and counter its disassembly by Wnt (Fig. 4D), thereby plateauing when equilibrium is achieved. This implies a safeguard mechanism by which rising concentrations of  $\beta$ -catenin could trigger its own degradation to avoid excessive accumulation. Axin

represents a scaffold with an on/off switch controlled through a ligand- and phosphorylation-dependent intramolecular interaction, which additionally could serve as a feedback sensor of target ( $\beta$ -catenin) concentrations. Similar scaffold functions could occur in other pathways as highlighted by yeast Ste5 (30).

**References and Notes**

1. B. T. MacDonald, K. Tamai, X. He, *Dev. Cell* **17**, 9 (2009).
2. H. Clevers, R. Nusse, *Cell* **149**, 1192 (2012).
3. C. Liu *et al.*, *Cell* **108**, 837 (2002).
4. J. Mao *et al.*, *Mol. Cell* **7**, 801 (2001).
5. K. Tamai *et al.*, *Mol. Cell* **13**, 149 (2004).
6. X. Zeng *et al.*, *Nature* **438**, 873 (2005).
7. G. Davidson *et al.*, *Nature* **438**, 867 (2005).
8. J. Bilic *et al.*, *Science* **316**, 1619 (2007).
9. X. Zeng *et al.*, *Development* **135**, 367 (2008).
10. T. Schwarz-Romond, C. Metcalfe, M. Bienz, *J. Cell Sci.* **120**, 2402 (2007).
11. C. Metcalfe, M. Bienz, *J. Cell Sci.* **124**, 3537 (2011).
12. S. Ikeda *et al.*, *EMBO J.* **17**, 1371 (1998).
13. J. Behrens *et al.*, *Science* **280**, 596 (1998).
14. D. Kimelman, W. Xu, *Oncogene* **25**, 7482 (2006).
15. J. L. Stamos, W. I. Weis, *Cold Spring Harb. Perspect. Biol.* **5**, a007898 (2013).
16. H. Yamamoto *et al.*, *J. Biol. Chem.* **274**, 10681 (1999).
17. K. Willert, S. Shibamoto, R. Nusse, *Genes Dev.* **13**, 1768 (1999).
18. E. Jho, S. Lomvardas, F. Costantini, *Biochem. Biophys. Res. Commun.* **266**, 28 (1999).
19. W. Luo *et al.*, *EMBO J.* **26**, 1511 (2007).
20. D. M. Virshup, S. Shenolikar, *Mol. Cell* **33**, 537 (2009).
21. C. Niehrs, *Nat. Rev. Genet.* **5**, 425 (2004).
22. V. S. W. Li *et al.*, *Cell* **149**, 1245 (2012).
23. V. F. Taelman *et al.*, *Cell* **143**, 1136 (2010).
24. A. R. Hernández, A. M. Klein, M. W. Kirschner, *Science* **338**, 1337 (2012).
25. A. J. Valvezan, F. Zhang, J. A. Diehl, P. S. Klein, *J. Biol. Chem.* **287**, 3823 (2012).
26. B. W. Doble, S. Patel, G. A. Wood, L. K. Kockeritz, J. R. Woodgett, *Dev. Cell* **12**, 957 (2007).
27. G. Wu, H. Huang, J. Garcia Abreu, X. He, *PLoS ONE* **4**, e9426 (2009).
28. C. S. Celenyi *et al.*, *Proc. Natl. Acad. Sci. U.S.A.* **105**, 8032 (2008).
29. S. Piao *et al.*, *PLoS ONE* **3**, e4046 (2008).
30. J. G. Zalatan, S. M. Coyle, S. Rajan, S. S. Sidhu, W. A. Lim, *Science* **337**, 1218 (2012).

**Acknowledgments:** We thank Y. Wu for the BCD2 construct; X. Yu for figs. S11 and S13; B. Doble and J. Woodgett for Gsk3-null mouse embryonic stem cells; A. Klein, M. Kirschner, T. Schwarz, J.-h. Wang, and X.H. laboratory members for comments; and M. Lin, B. Yu, M. Wan, X. Cao, and W. Wei for help. S.-E.K. and H.H. were supported partially by postdoctoral fellowships from National Research Foundation of Korea (KRF-2009-357-C00096) and Canadian Institute of Health Research, respectively. J.G.A. was funded partially by the National Council for Scientific and Technological Development (CNPq, Brazil) as a visiting scientist to the X.H. laboratory. L.P. acknowledges support by NIH (R01EB008737 and R01EB015481). X.H. acknowledges support by NIH (R01 GM074241) and Boston Children’s Hospital Intellectual and Developmental Disabilities Research Center (P30 HD-18655).

**Supplementary Materials**

www.sciencemag.org/cgi/content/full/science.1232389/DC1  
Materials and Methods  
Figs. S1 to S18  
References (31–39)

5 November 2012; accepted 19 March 2013  
Published online 11 April 2013;  
10.1126/science.1232389